New Journal of Chemistry

Electronic Supplementary Information

for

Dinuclear aluminum complexes bearing methylene-bridged phenoxy-imine ligands and their application in the ring-opening polymerization of *rac*-lactide

Nattawut Yuntawattana, Chutikan Nakhonkhet, Tanin Nanok, Kanokon Upitak,

and Pimpa Homnirun*

Laboratory of Catalysts and Advanced Polymer Materials, Department of Chemistry and Center of Excellence for Innovation in Chemistry, Faculty of Science, Kasetsart University, Bangkok 10900, Thailand

*E-mail: fscipph@ku.ac.th

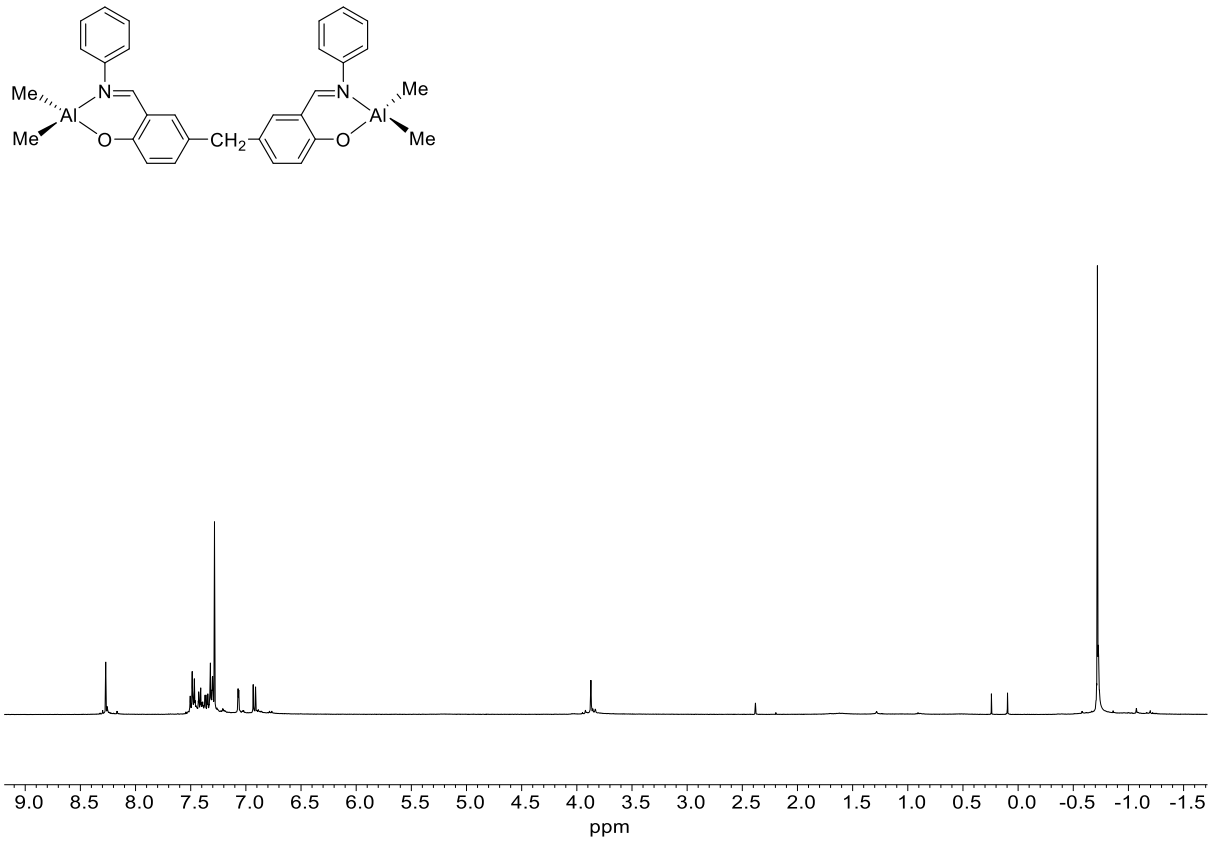

Fig. S1 ^{1}H NMR spectrum of **1** in $CDCl_3$ at 298 K.

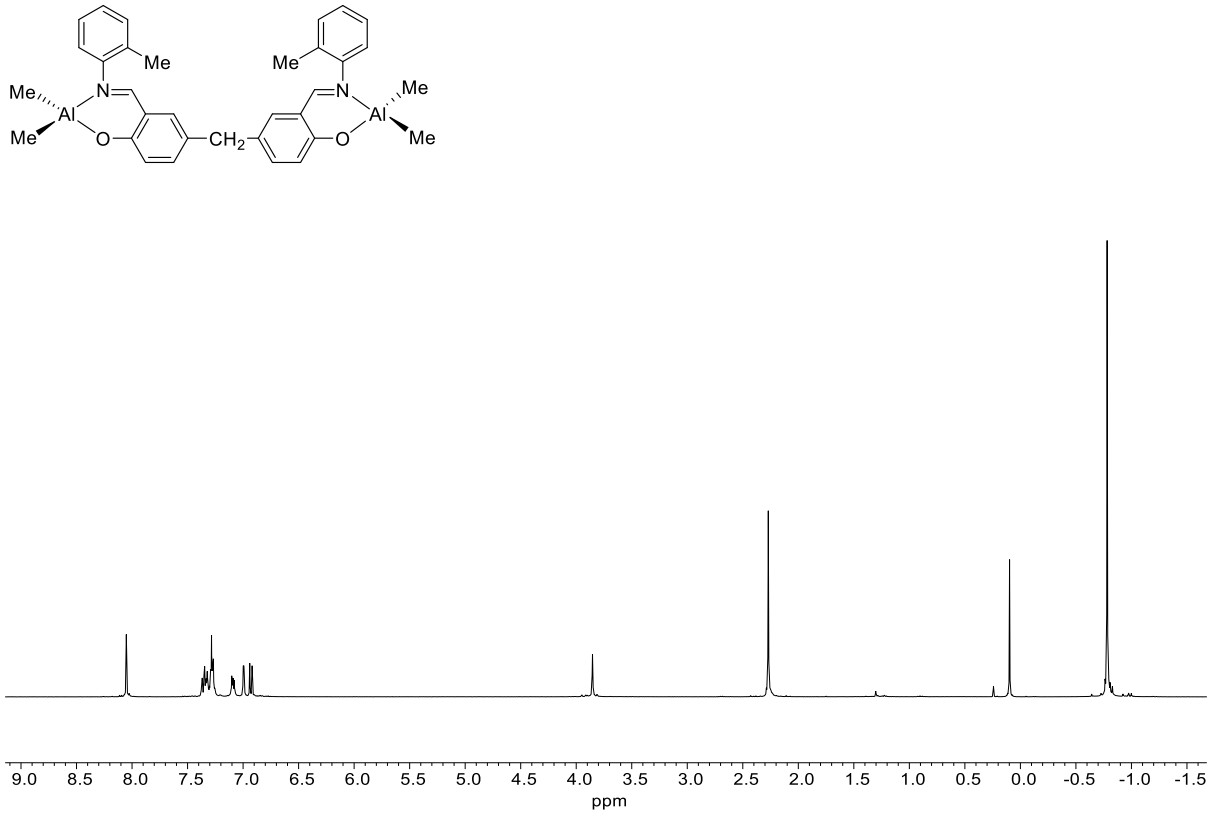

Fig. S2 ^{1}H NMR spectrum of **2** in $CDCl_3$ at 298 K.

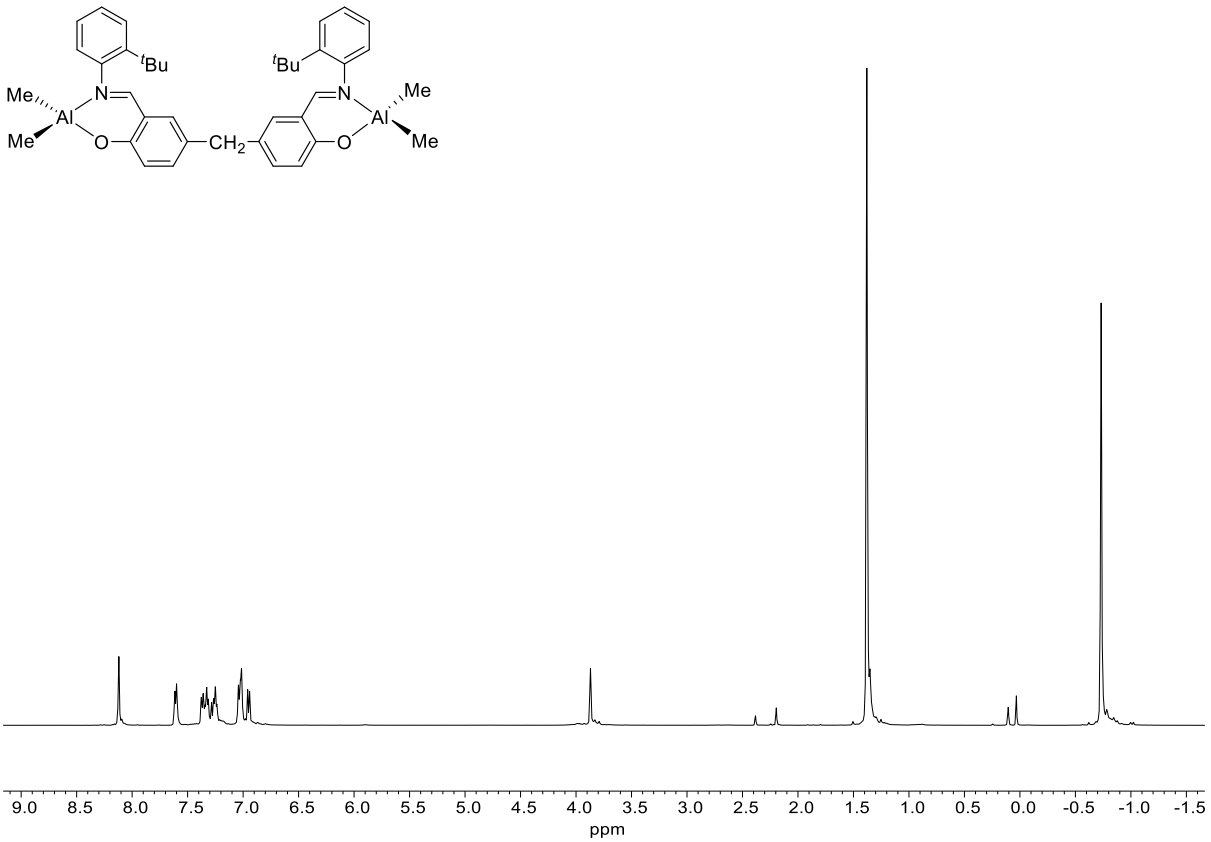

Fig. S3 ^{1}H NMR spectrum of **3** in $CDCl_3$ at 298 K.

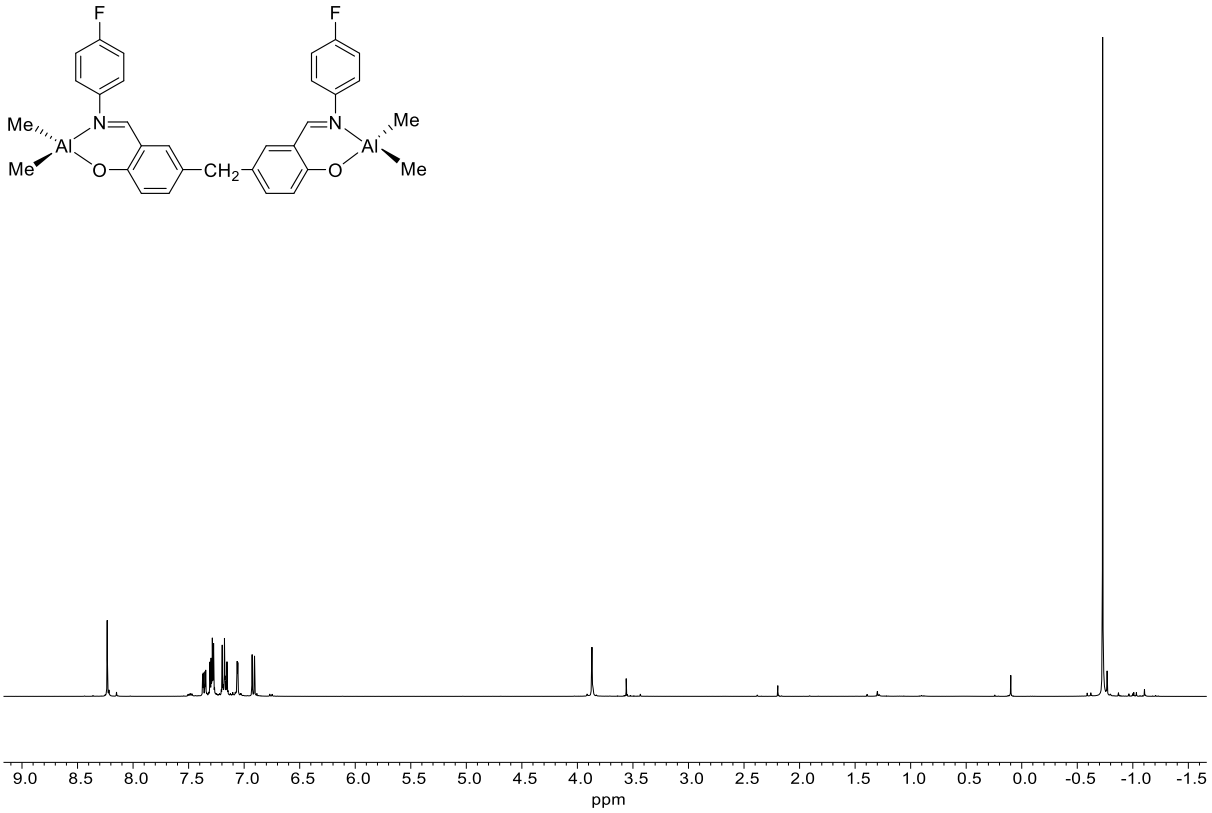

Fig. S4 ^{1}H NMR spectrum of **4** in $CDCl_3$ at 298 K.

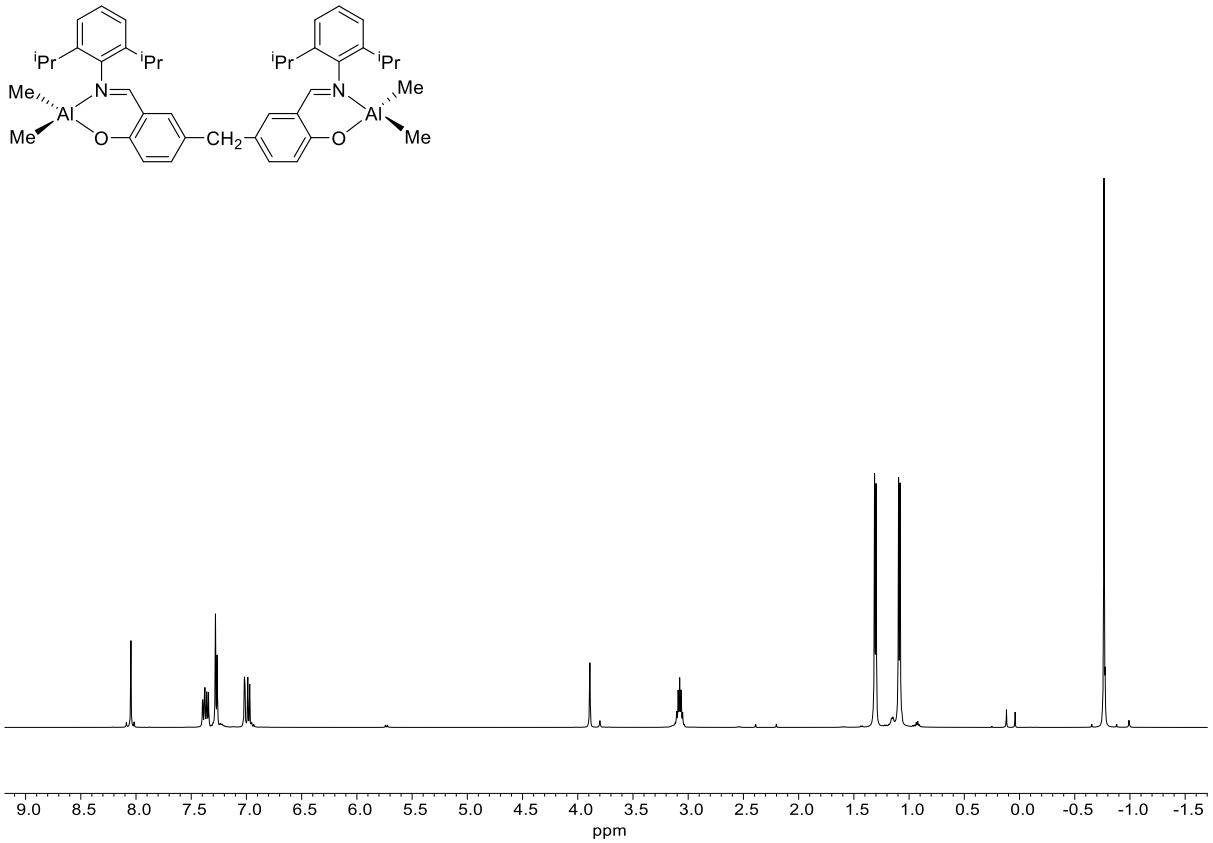

Fig. S5 ^{1}H NMR spectrum of **5** in $CDCl_3$ at 298 K.

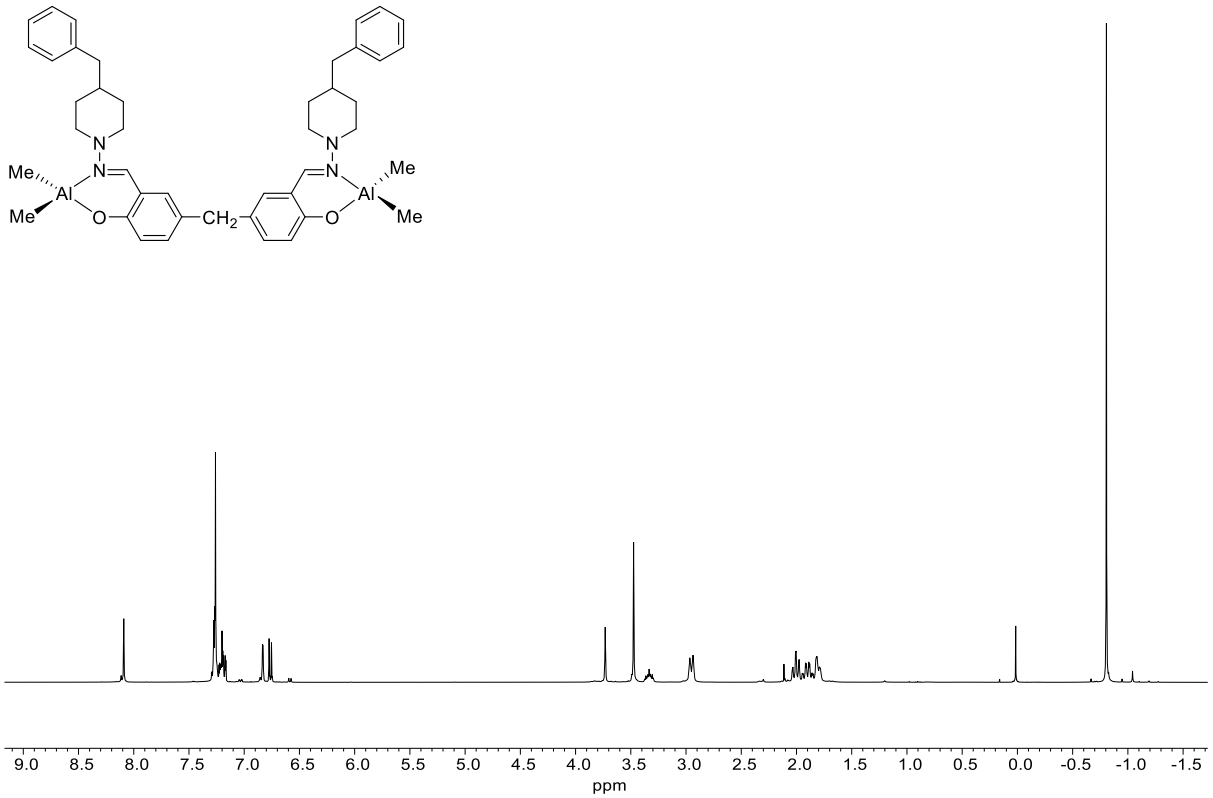

Fig. S6 ^{1}H NMR spectrum of **6** in $CDCl_3$ at 298 K.

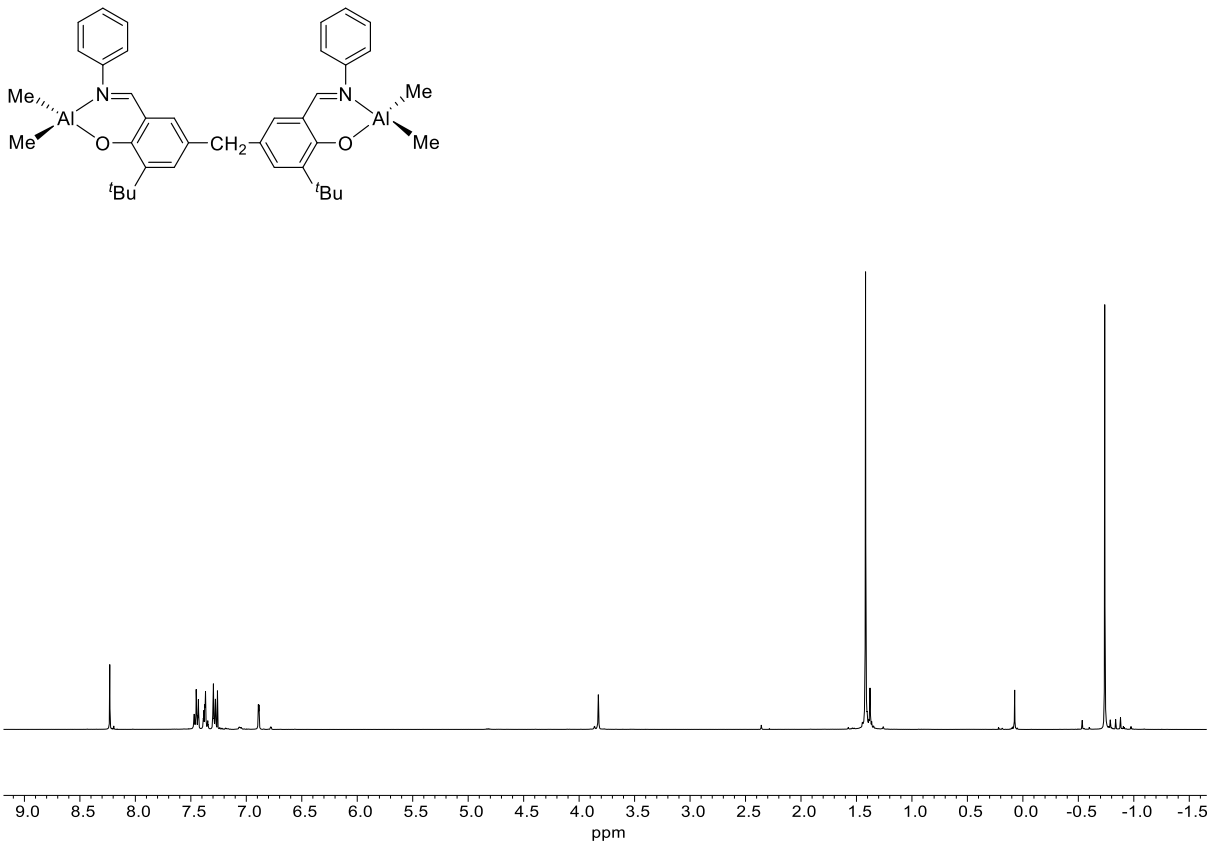

Fig. S7 ^{1}H NMR spectrum of **7** in $CDCl_3$ at 298 K.

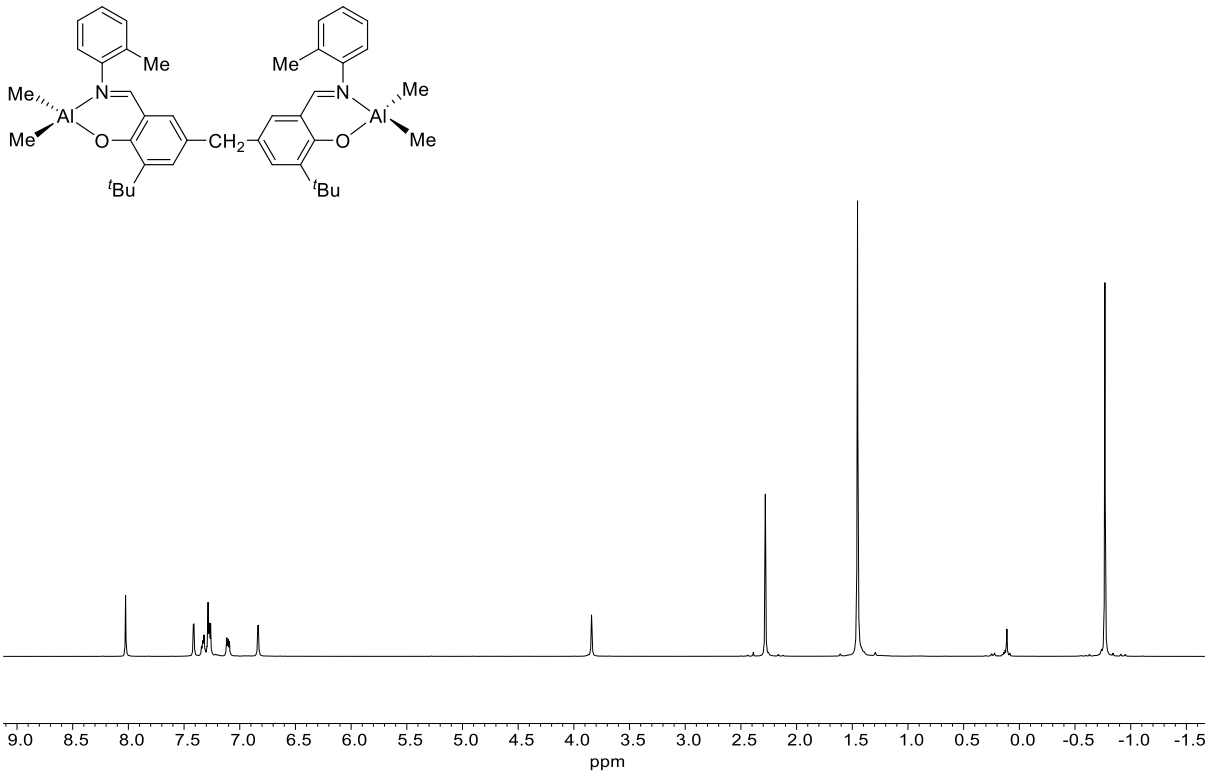

Fig. S8 ^{1}H NMR spectrum of **8** in $CDCl_3$ at 298 K.

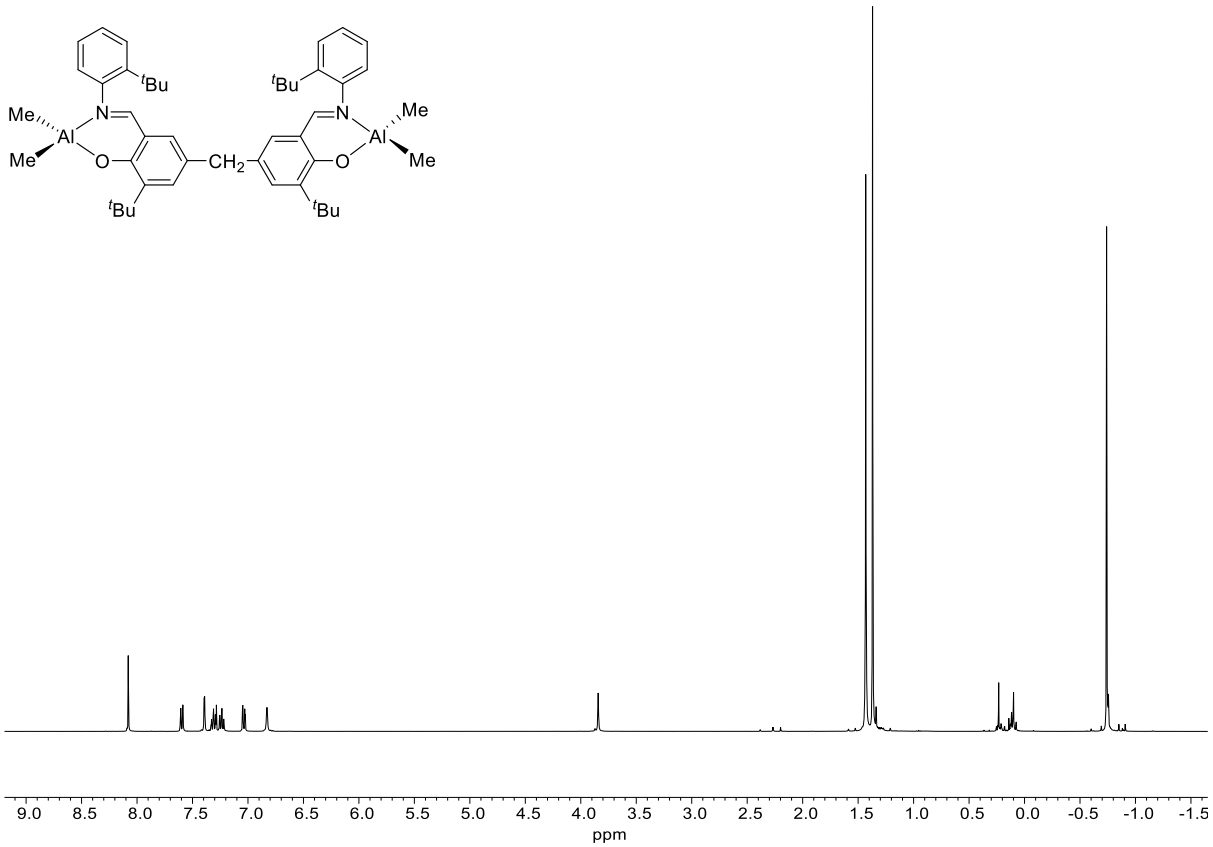

Fig. S9 ^{1}H NMR spectrum of **9** in $CDCl_3$ at 298 K.

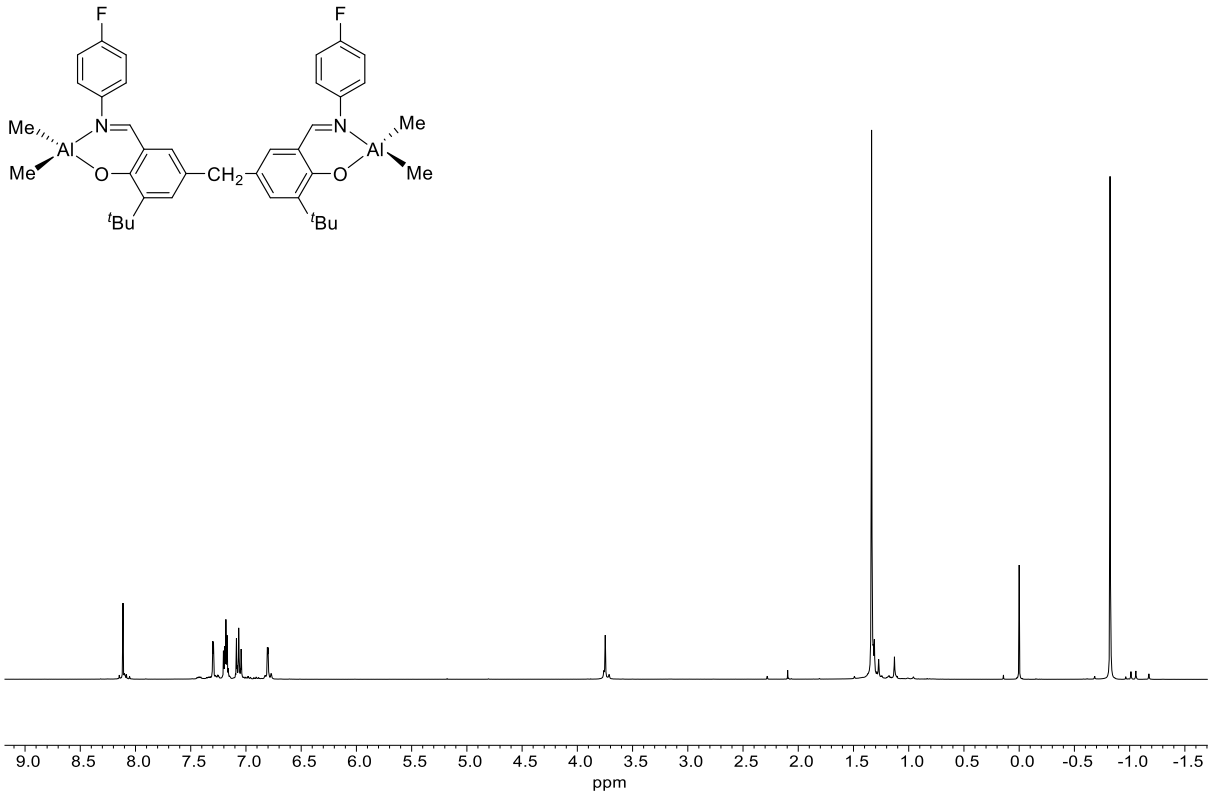

Fig. S10 ^{1}H NMR spectrum of **10** in $CDCl_3$ at 298 K.

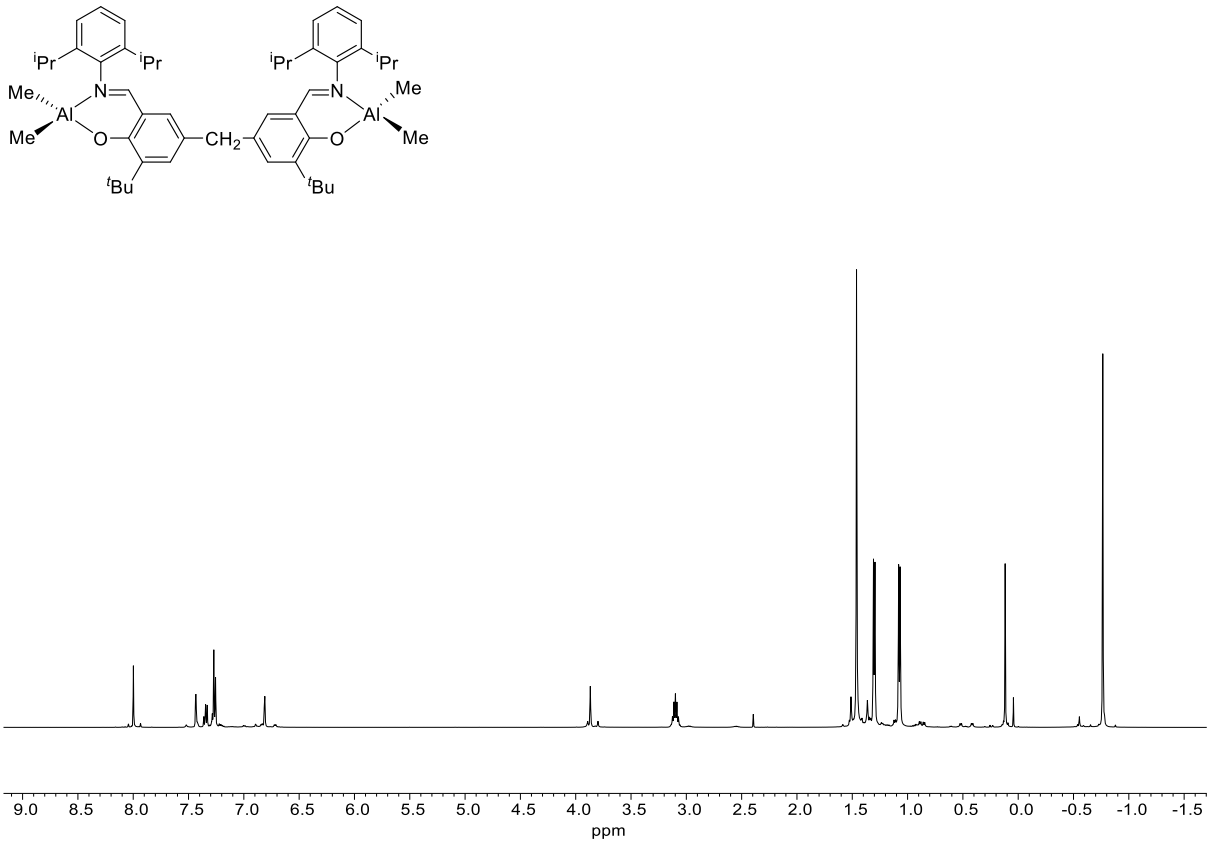

Fig. S11 ^{1}H NMR spectrum of **11** in $CDCl_3$ at 298 K.

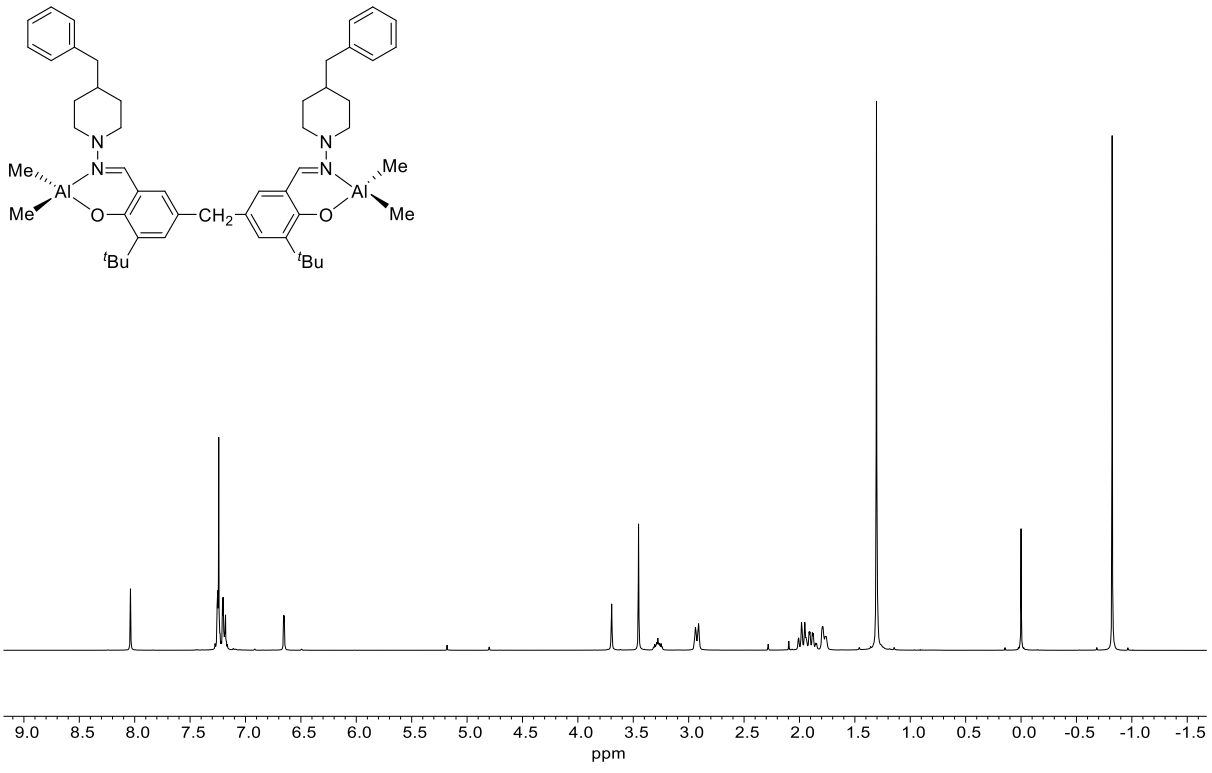

Fig. S12 ^{1}H NMR spectrum of **12** in $CDCl_3$ at 298 K.

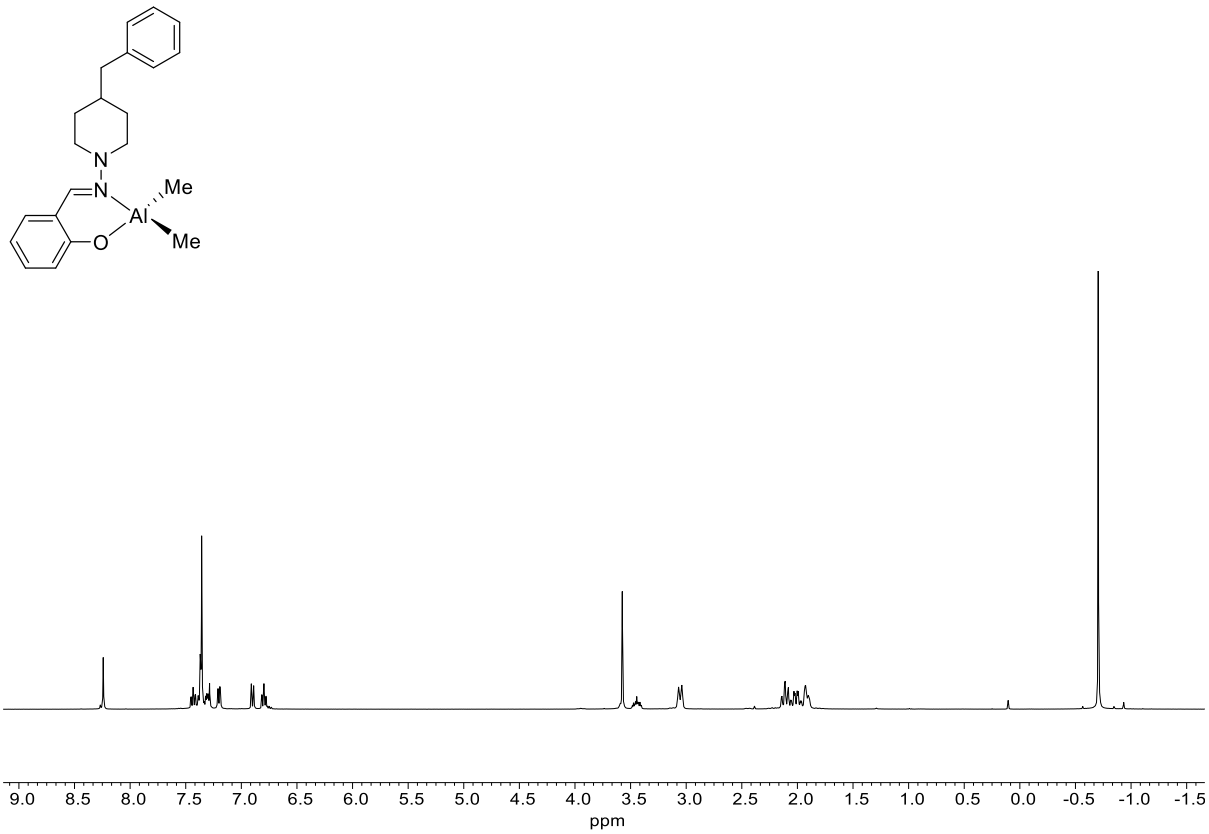

Fig. S13 ^{1}H NMR spectrum of **13** in $CDCl_3$ at 298 K.

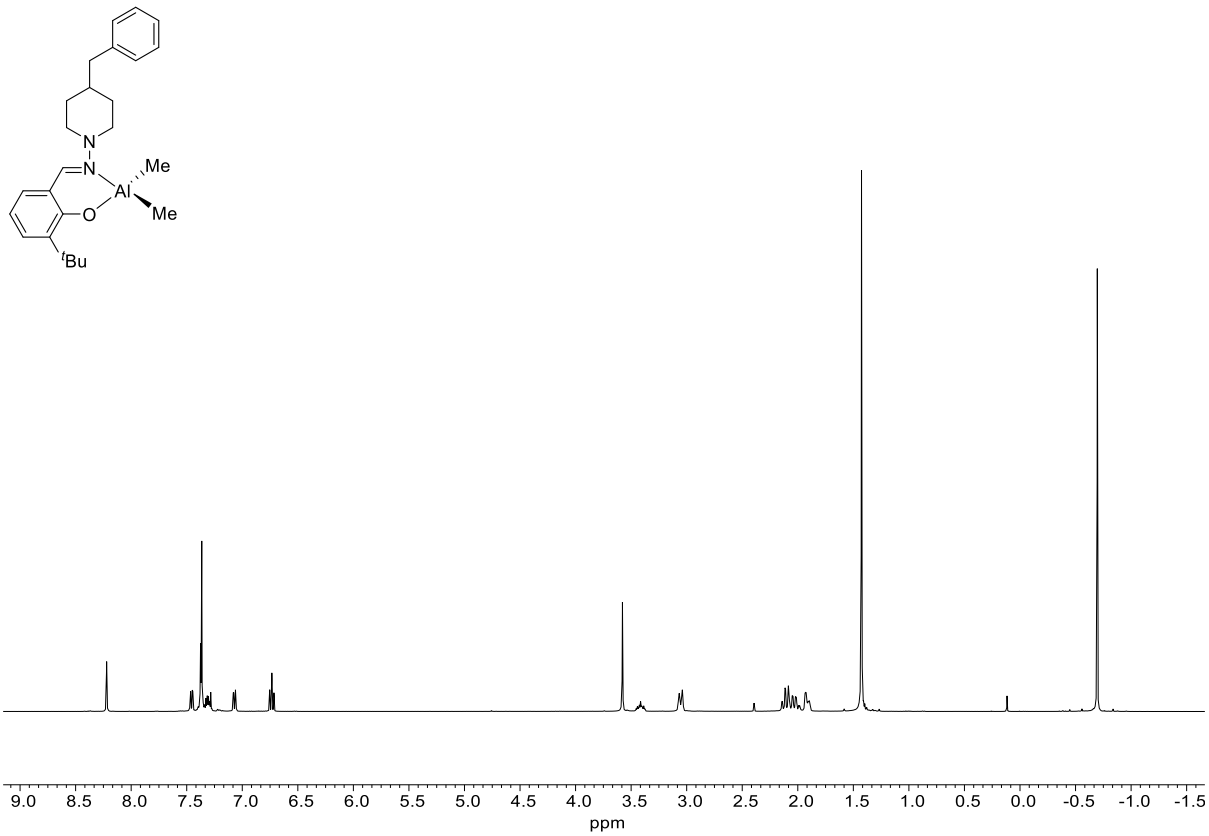

Fig. S14 ^{1}H NMR spectrum of **14** in $CDCl_3$ at 298 K.

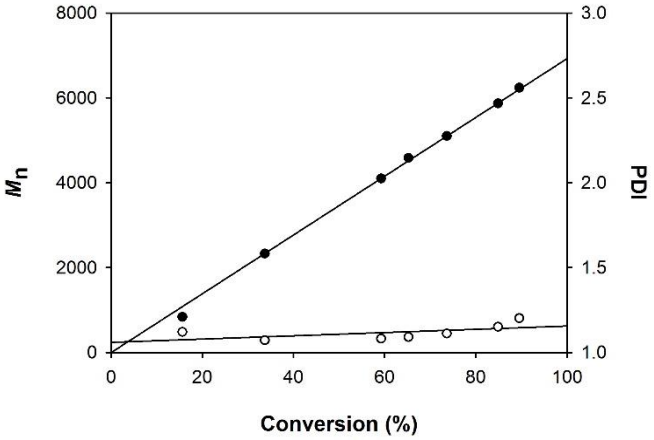

Fig. S15 Plot of PLA M_n (●) and PDI (○) as a function of monomer conversion for a *rac*-LA polymerization using **2**/BnOH ($[LA]_0$:$[Int]_0$:$[BnOH]_0$ = 100:1:2, toluene, 70 ºC).

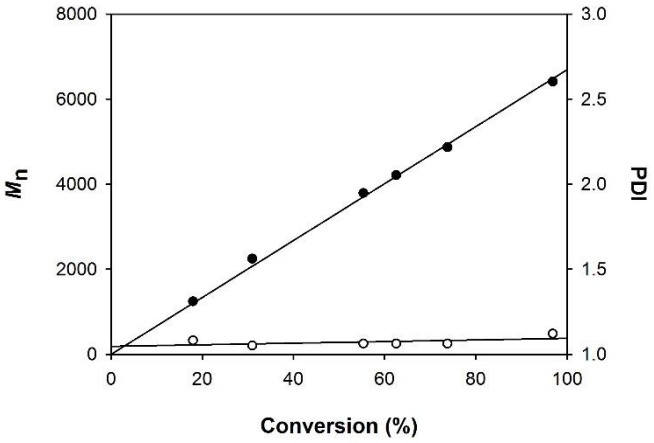

Fig. S16 Plot of PLA M_n (●) and PDI (○) as a function of monomer conversion for a *rac*-LA polymerization using **3**/BnOH ($[LA]_0$:$[Int]_0$:$[BnOH]_0$] = 100:1:2, toluene, 70 ºC).

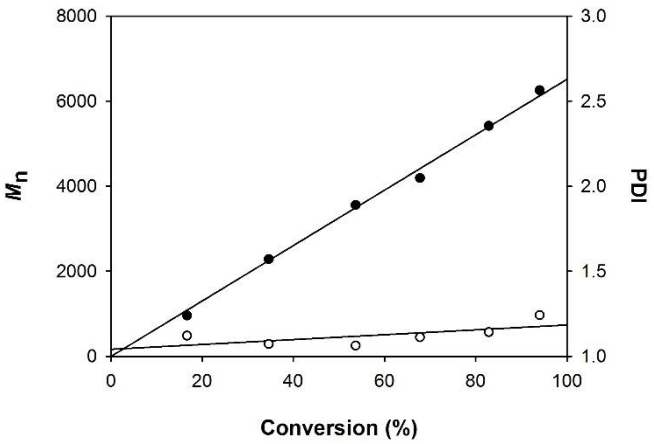

Fig. S17 Plot of PLA M_n (●) and PDI (○) as a function of monomer conversion for a *rac*-LA polymerization using **4**/BnOH ($[LA]_0$:$[Int]_0$:$[BnOH]_0$ = 100:1:2, toluene, 70 ºC).

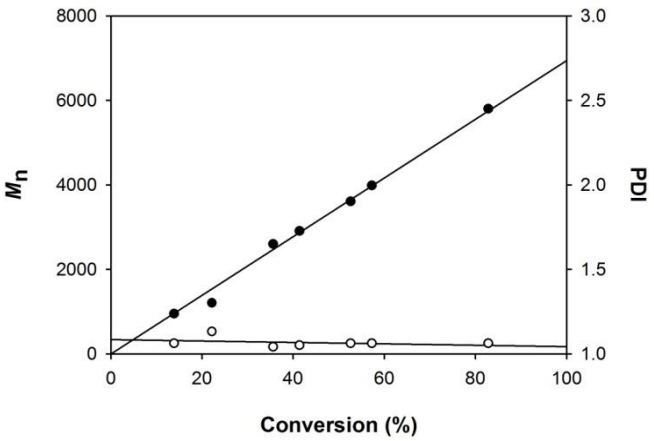

Fig. S18 Plot of PLA M_n (●) and PDI (○) as a function of monomer conversion for a *rac*-LA polymerization using **5**/BnOH ($[LA]_0$:$[Int]_0$:$[BnOH]_0$ = 100:1:2, toluene, 70 ºC).

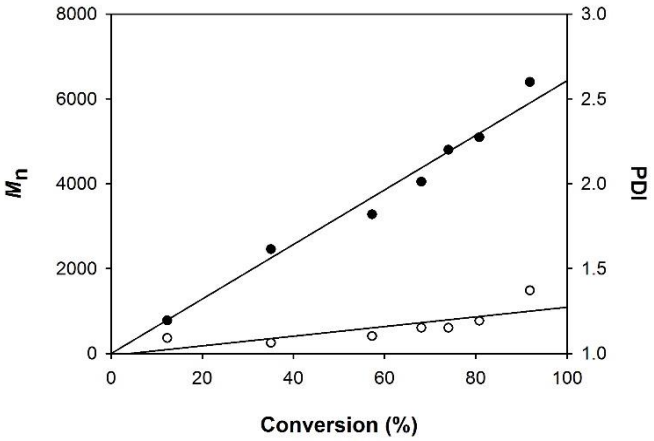

Fig. S19 Plot of PLA M_n (●) and PDI (○) as a function of monomer conversion for a *rac*-LA polymerization using **6**/BnOH ($[LA]_0$:$[Int]_0$:$[BnOH]_0$ = 100:1:2, toluene, 70 ºC).

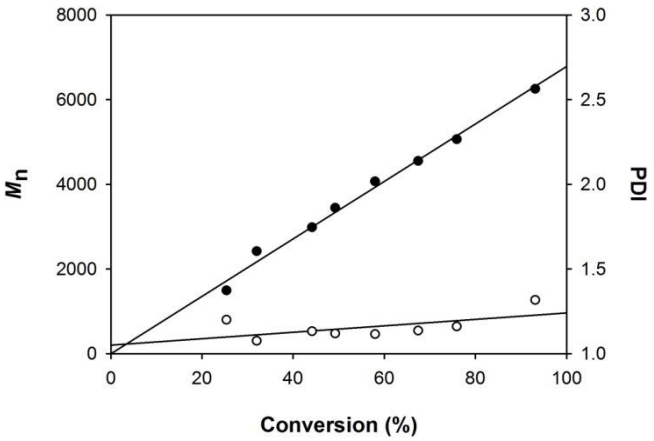

Fig. S20 Plot of PLA M_n (●) and PDI (○) as a function of monomer conversion for a *rac*-LA polymerization using **7**/BnOH ($[LA]_0$:$[Int]_0$:$[BnOH]_0$ = 100:1:2, toluene, 70 ºC).

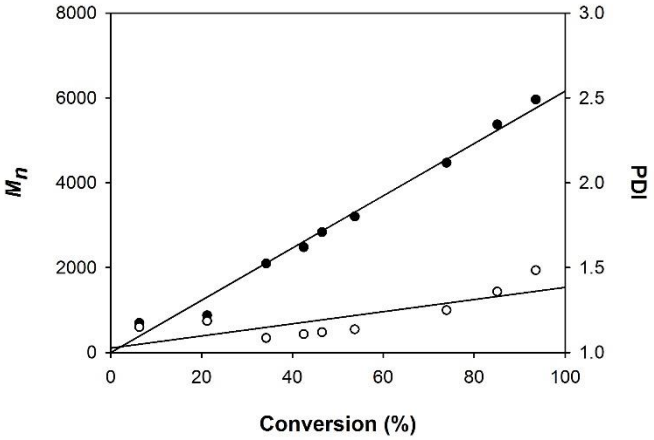

Fig. S21 Plot of PLA M_n (●) and PDI (○) as a function of monomer conversion for a *rac*-LA polymerization using **8**/$PhCH_2OH$ ($[LA]_0$:$[Int]_0$:$[BnOH]_0$ = 100:1:2, toluene, 70 ºC).

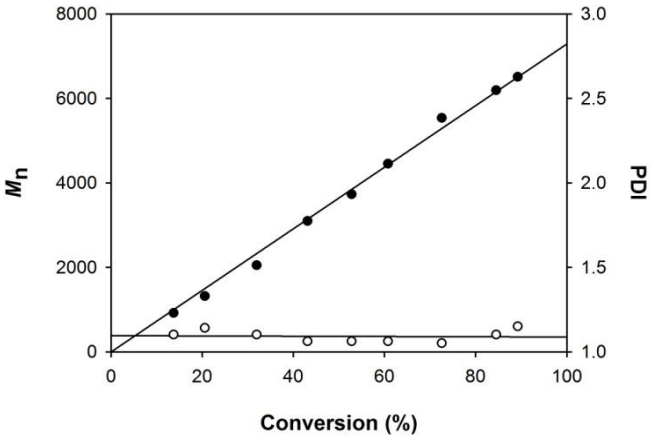

Fig. S22 Plot of PLA M_n (●) and PDI (○) as a function of monomer conversion for a *rac*-LA polymerization using **9**/BnOH ($[LA]_0$:$[Int]_0$:$[BnOH]_0$ = 100:1:2, toluene, 70 ºC).

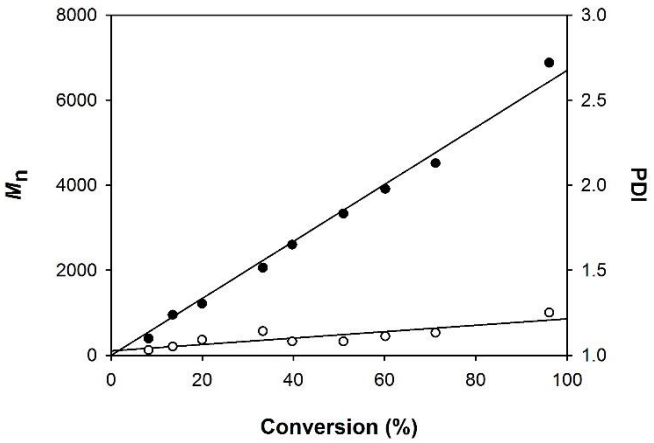

Fig. S23 Plot of PLA M_n (●) and PDI (○) as a function of monomer conversion for a *rac*-LA polymerization using **10**/BnOH ($[LA]_0$:$[Int]_0$:$[BnOH]_0$ = 100:1:2, toluene, 70 ºC).

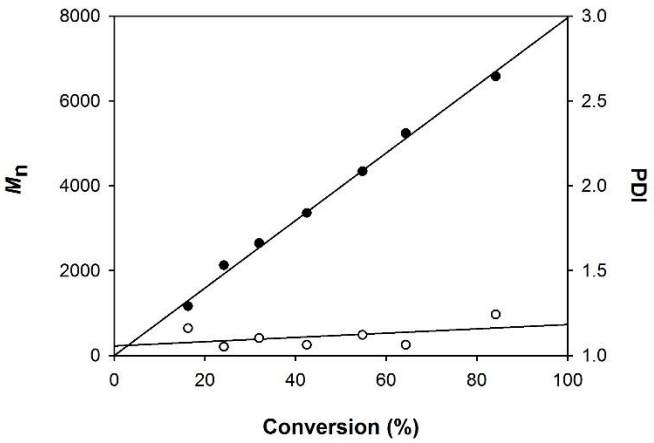

Fig. S24 Plot of PLA M_n (●) and PDI (○) as a function of monomer conversion for a *rac*-LA polymerization using **11**/BnOH ($[LA]_0$:$[Int]_0$:$[BnOH]_0$ = 100:1:2, toluene, 70 ºC).

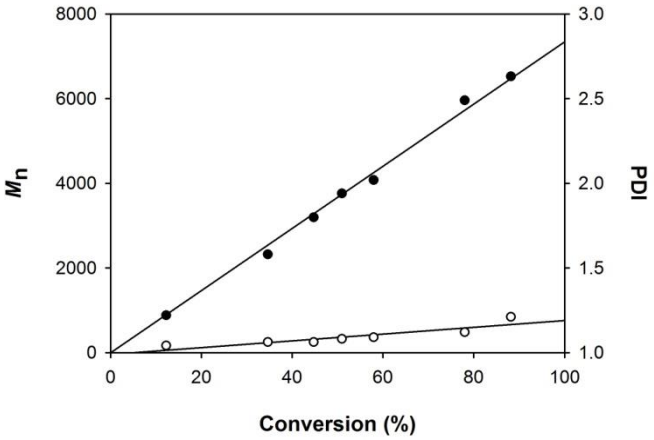

Fig. S25 Plot of PLA M_n (●) and PDI (○) as a function of monomer conversion for a *rac*-LA polymerization using **12**/BnOH ($[LA]_0$:$[Int]_0$:$[BnOH]_0$ = 100:1:2, toluene, 70 ºC).

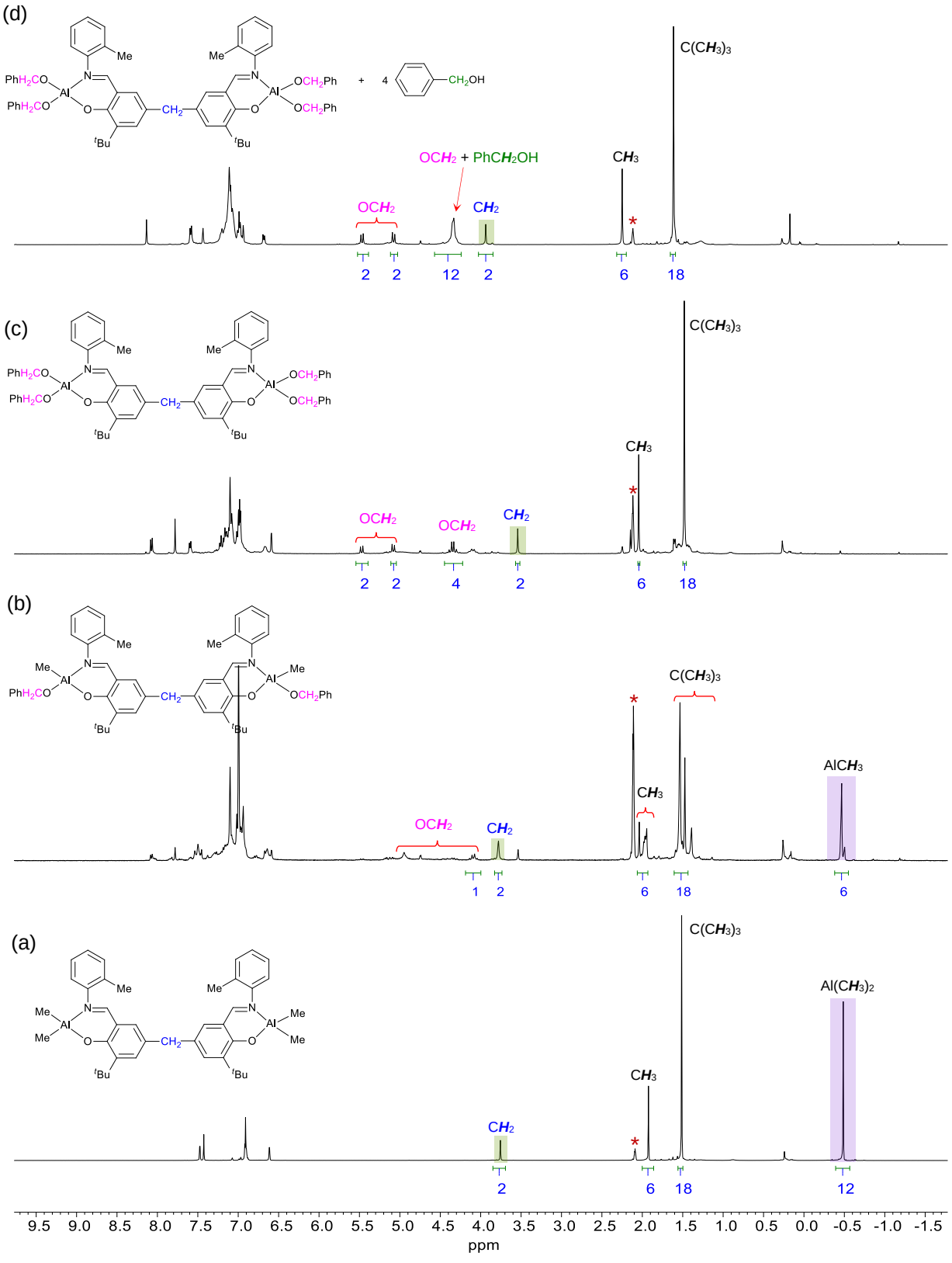

Fig. S26 ^{1}H NMR spectra of (a) complex **8**, (b) complex **8** + 2 eq. BnOH ($[Int]_0$:$[BnOH]_0$ = 1:2) (c) complex **8** + 4 eq. BnOH ($[Int]_0$:$[BnOH]_0$ = 1:4), and (d) complex **8** + 8 eq. BnOH ($[Int]_0$:$[BnOH]_0$ = 1:8) in d^8-toluene at 70 °C (* = d^8-toluene).

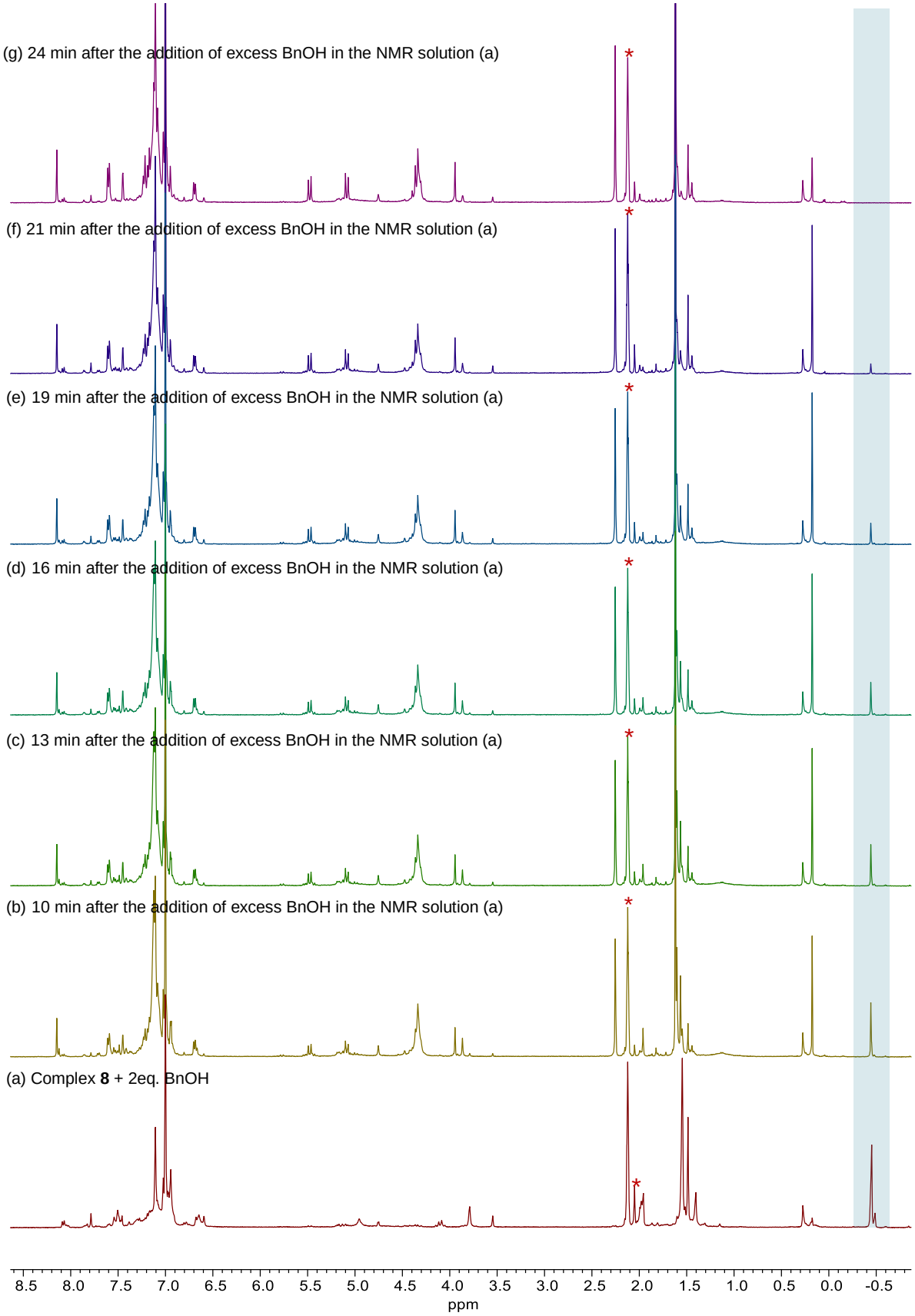

Fig. S27 ^{1}H NMR spectra of (a) the reaction mixture of complex **8** and 2 equivalents of BnOH, (b) 10 min (c) 13 min, (d) 16 min, (e) 19 min, (f) 21 min, (g) 24 min after the addtion of excess about of BnOH into the NMR solution of (a) in d^8-toluene at 70 °C (* = d^8-toluene).

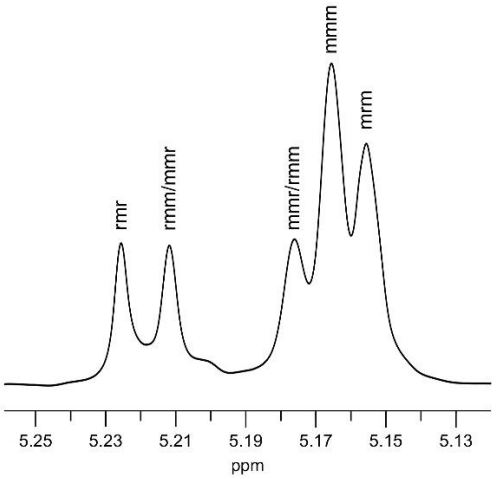

Fig. S28 Homonuclear decoupled ^{1}H NMR spectrum of the methine region of PLA prepared from *rac*-LA at 70 °C in toluene (500 MHz, $CDCl_3$) with complex **1**/BnOH.

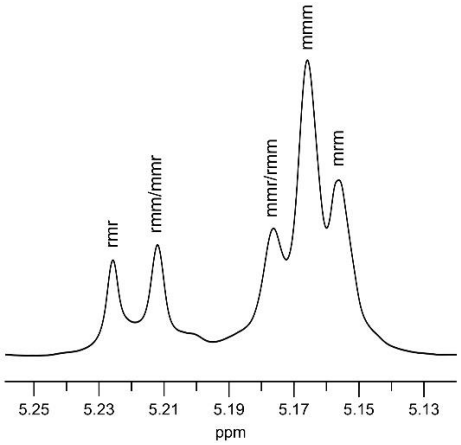

Fig. S29 Homonuclear decoupled ^{1}H NMR spectrum of the methine region of PLA prepared from *rac*-LA at 70 °C in toluene (500 MHz, $CDCl_3$) with complex **2**/BnOH.

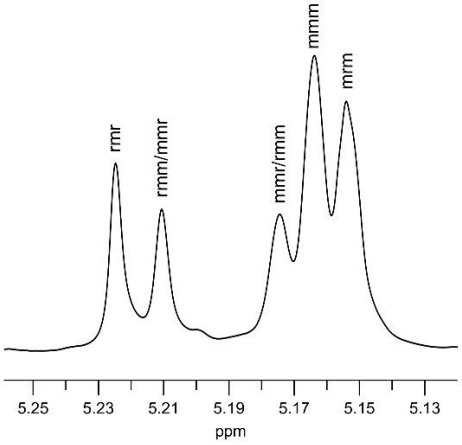

Fig. S30 Homonuclear decoupled ^{1}H NMR spectrum of the methine region of PLA prepared from *rac*-LA at 70 °C in toluene (500 MHz, $CDCl_3$) with complex **3**/BnOH.

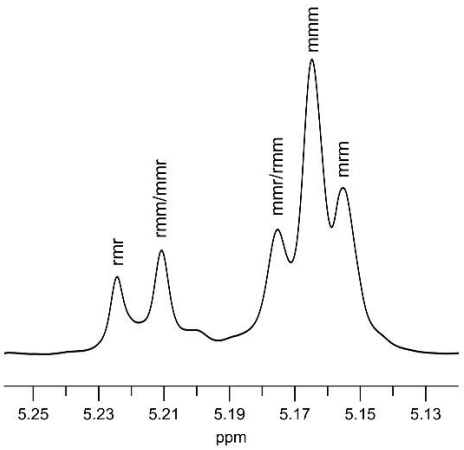

Fig. S31 Homonuclear decoupled ^{1}H NMR spectrum of the methine region of PLA prepared from *rac*-LA at 70 °C in toluene (500 MHz, $CDCl_3$) with complex **4**/BnOH.

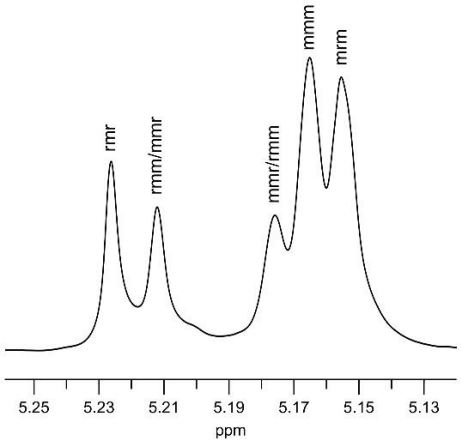

Fig. S32 Homonuclear decoupled ^{1}H NMR spectrum of the methine region of PLA prepared from *rac*-LA at 70 °C in toluene (500 MHz, $CDCl_3$) with complex **5**/BnOH.

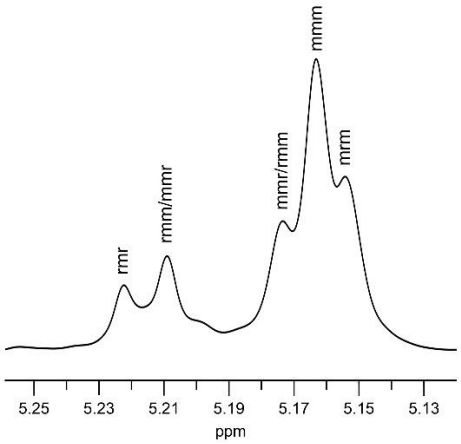

Fig. S33 Homonuclear decoupled ^{1}H NMR spectrum of the methine region of PLA prepared from *rac*-LA at 70 °C in toluene (500 MHz, $CDCl_3$) with complex **6**/BnOH.

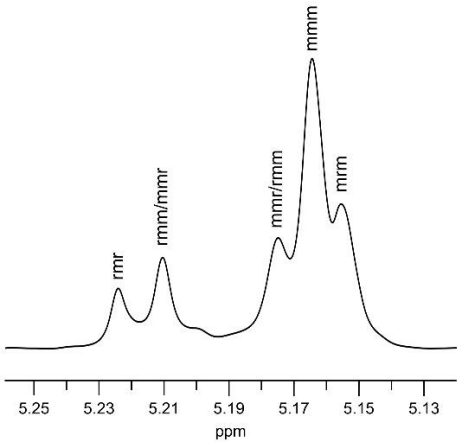

Fig. S34 Homonuclear decoupled ^{1}H NMR spectrum of the methine region of PLA prepared from *rac*-LA at 70 °C in toluene (500 MHz, $CDCl_3$) with complex **7**/BnOH.

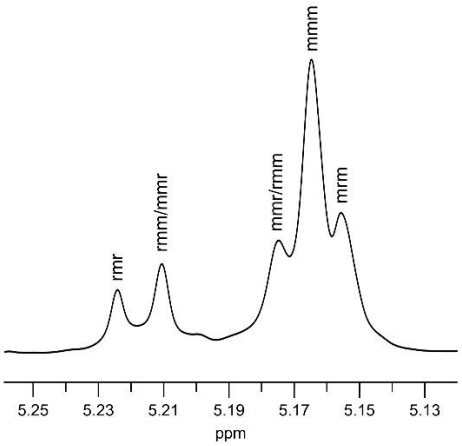

Fig. S35 Homonuclear decoupled ^{1}H NMR spectrum of the methine region of PLA prepared from *rac*-LA at 70 °C in toluene (500 MHz, $CDCl_3$) with complex **8**/BnOH.

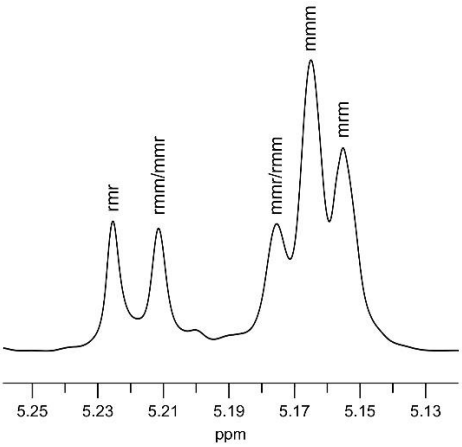

Fig. S36 Homonuclear decoupled ^{1}H NMR spectrum of the methine region of PLA prepared from *rac*-LA at 70 °C in toluene (500 MHz, $CDCl_3$) with complex **9**/BnOH.

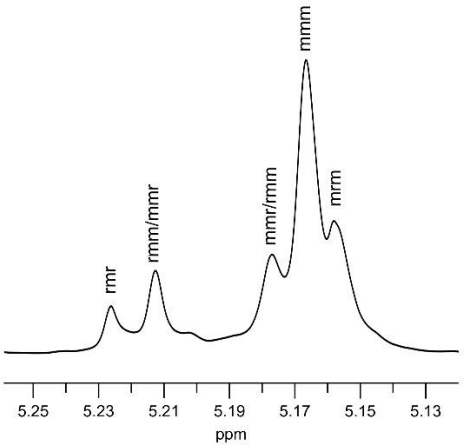

Fig. S37 Homonuclear decoupled ^{1}H NMR spectrum of the methine region of PLA prepared from *rac*-LA at 70 °C in toluene (500 MHz, $CDCl_3$) with complex **10**/BnOH.

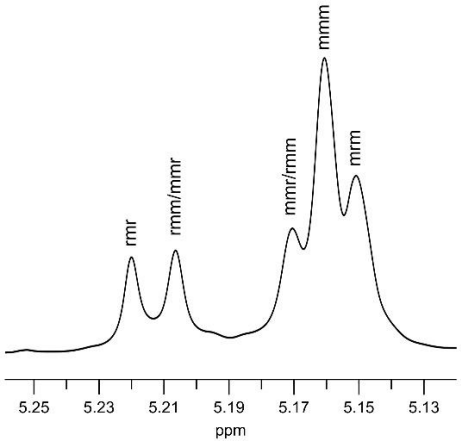

Fig. S38 Homonuclear decoupled ^{1}H NMR spectrum of the methine region of PLA prepared from *rac*-LA at 70 °C in toluene (500 MHz, $CDCl_3$) with complex **11**/BnOH.

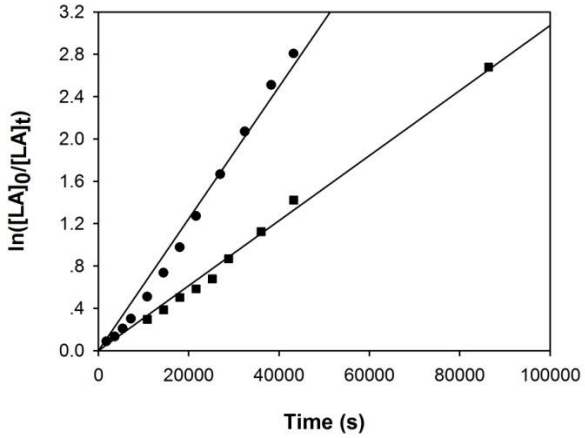

Fig. S39 Semilogarithmic plots of *rac*-lactide conversion *versus* time in toluene at 70 ºC with complexes **1** (●) and **7** (■) ($[LA]_0$:$[Int]_0$:$[BnOH]_0$ = 100:1:2, $[LA]_0$ = 0.83 M, $[Int]_0$ = 8.33 mM).

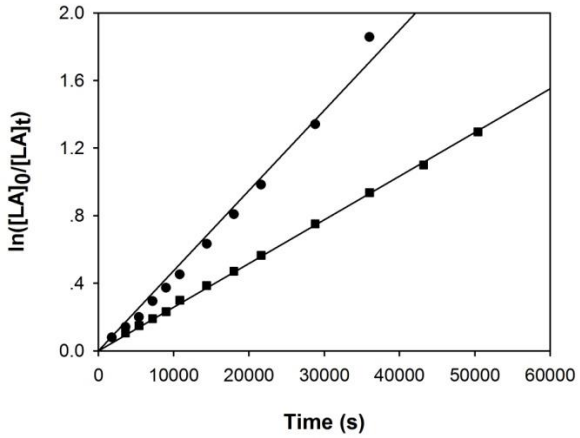

Fig. S40 Semilogarithmic plots of *rac*-lactide conversion *versus* time in toluene at 70 ºC with complexes **3** (●) and **9** (■) ([[LA]$_0$:[Int]$_0$:[BnOH]$_0$ = 100:1:2, [LA]$_0$ = 0.83 M, [Int]$_0$ = 8.33 mM).

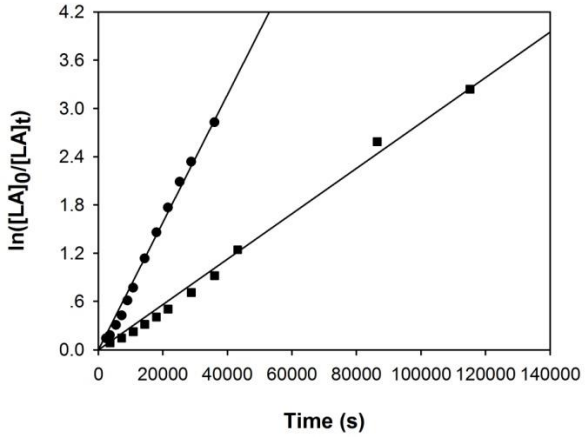

Fig. S41 Semilogarithmic plots of *rac*-lactide conversion *versus* time in toluene at 70 ºC with complexes **4** (●) and **10** (■) ([LA]$_0$:[Int]$_0$:[BnOH]$_0$ = 100:1:2, [LA]$_0$ = 0.83 M, [Int]$_0$ = 8.33 mM).

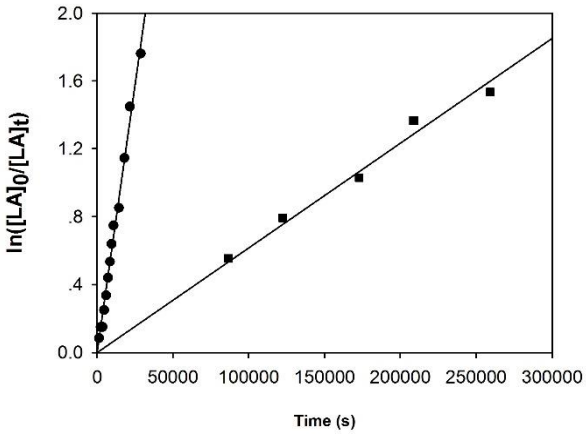

Fig. S42 Semilogarithmic plots of *rac*-lactide conversion *versus* time in toluene at 70 ºC with complexes **5** (●) and **11** (■) ([LA]$_0$:[Int]$_0$:[BnOH]$_0$ = 100:1:2, [LA]$_0$ = 0.83 M, [Int]$_0$ = 8.33 mM).

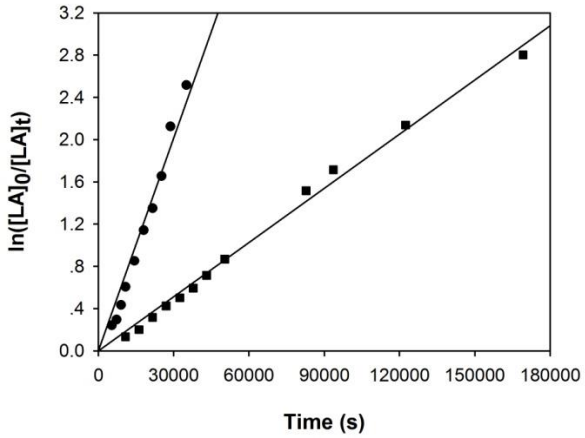

Fig. S43 Semilogarithmic plots of *rac*-lactide conversion *versus* time in toluene at 70 ºC with complexes **6** (●) and **12** (■) ($[LA]_0$:$[Int]_0$:$[BnOH]_0$ = 100:1:2, $[LA]_0$ = 0.83 M, $[Int]_0$ = 8.33 mM).

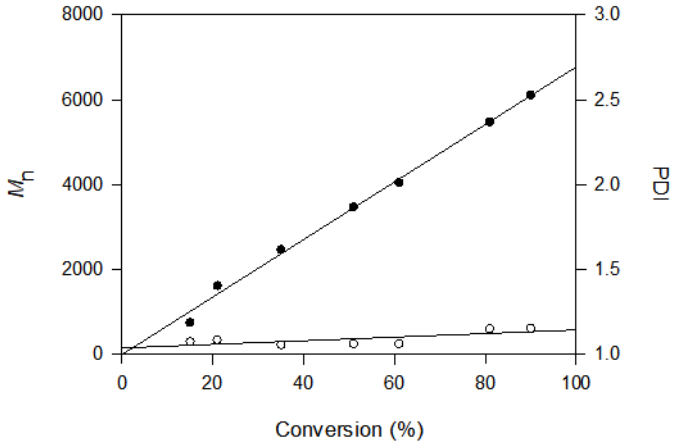

Fig. S44 Plot of PLA M_n (●) and PDI (○) as a function of monomer conversion for a *rac*-LA polymerization using **13**/BnOH ($[LA]_0$:$[Int]_0$:$[BnOH]_0$ = 50:1:1, toluene, 70 ºC).

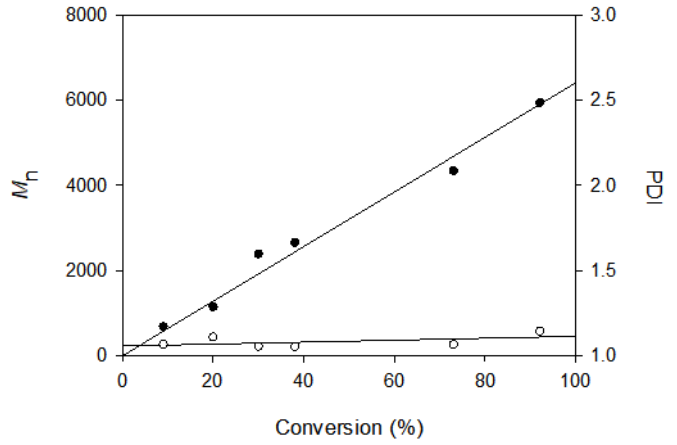

Fig. S45 Plot of PLA M_n (●) and PDI (○) as a function of monomer conversion for a *rac*-LA polymerization using **14**/BnOH ($[LA]_0$:$[Int]_0$:$[BnOH]_0$ = 50:1:1, toluene, 70 ºC).

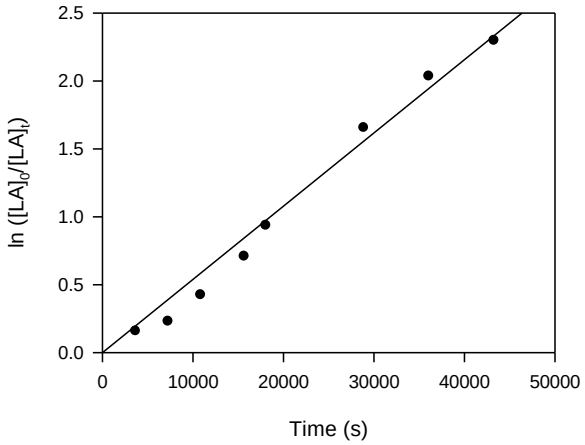

Fig. S46 Semilogarithmic plots of *rac*-LA conversion *versus* time in toluene at 70 ºC with complex **13** (●) ($[LA]_0$:$[Int]_0$:$[BnOH]_0$ = 50:1:1, $[LA]_0$ = 0.42 M, $[Int]_0$ = 8.33 mM).

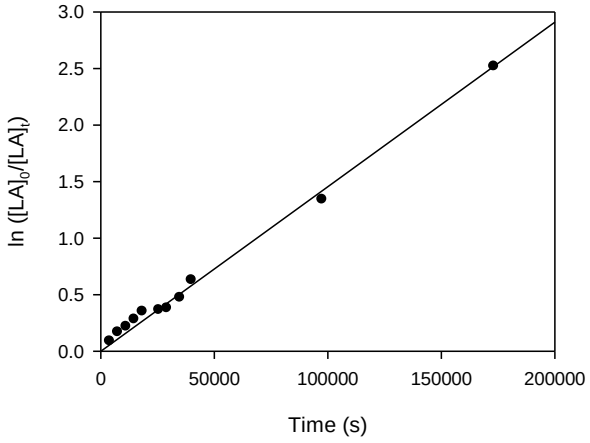

Fig. S47 Semilogarithmic plots of *rac*-LA conversion *versus* time in toluene at 70 ºC with complex **13** (●) ($[LA]_0$:$[Int]_0$:$[BnOH]_0$ = 50:1:1, $[LA]_0$ = 0.42 M, $[Int]_0$ = 8.33 mM).

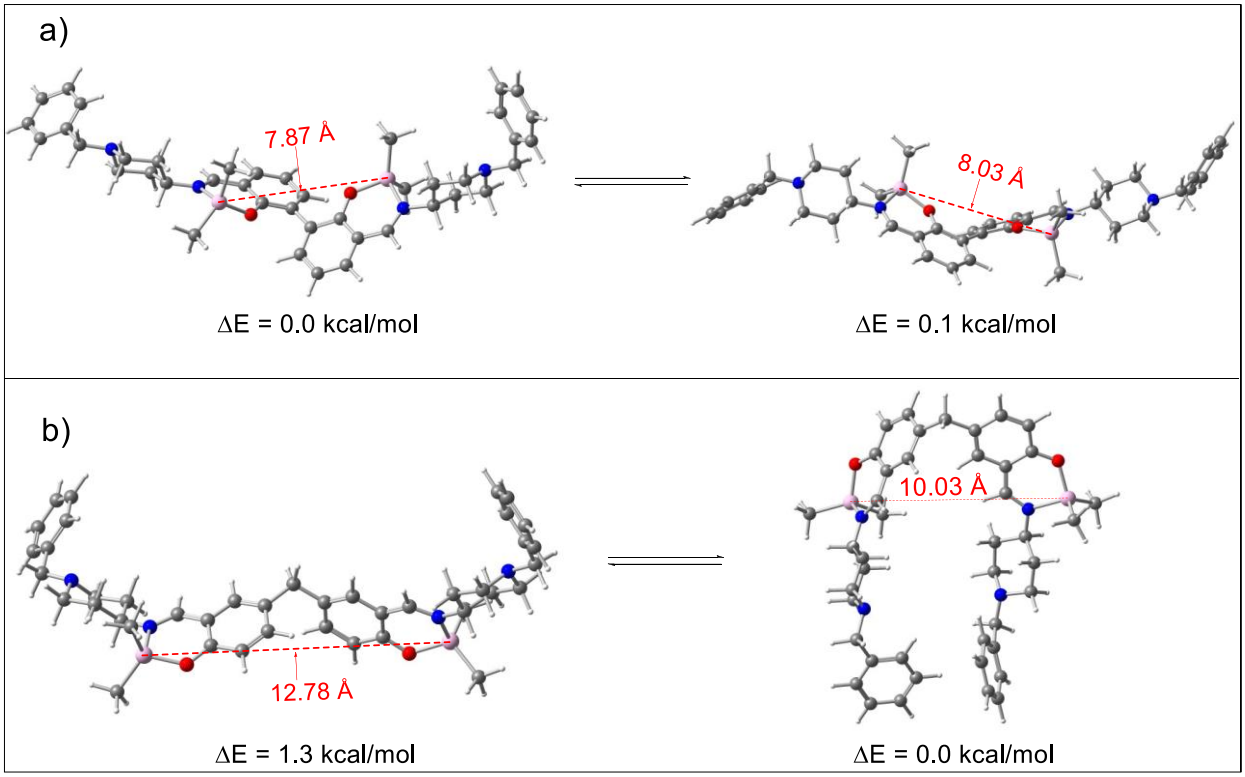

Fig. S48 Al-Al distances in two configurations of complexes **I** (a) and **6** (b) optimized at the M06-2X/6-311G(d,p) method.

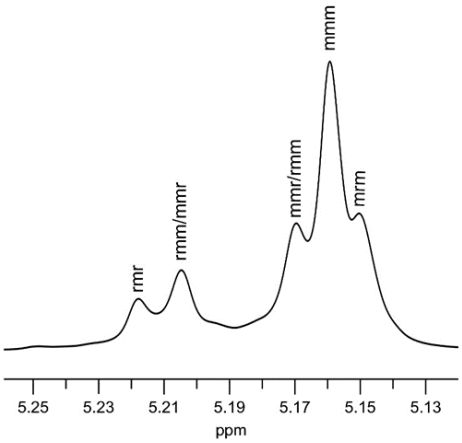

Fig. S49 Homonuclear decoupled ^{1}H NMR spectrum of the methine region of PLA prepared from *rac*-LA at 70 °C in toluene (500 MHz, $CDCl_3$) with complex **13**/BnOH.

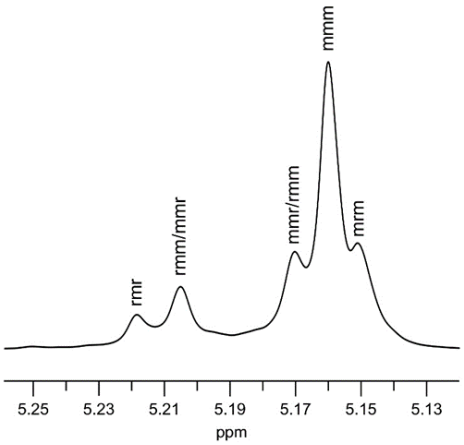

Fig. S50 Homonuclear decoupled ^{1}H NMR spectrum of the methine region of PLA prepared from *rac*-LA at 70 °C in toluene (500 MHz, $CDCl_3$) with complex **14**/BnOH.

Computational details

All geometry optimizations were carried out in the gas phase without molecular symmetry constraints using the hybrid meta exchange-correlation functional with double the amount of nonlocal exchange[1-3] (M06-2X) level of theory as implemented in the Gaussian09 program package.[4] The standard all-electron Pople basis set 6-311G(d,p) was applied to all atoms in the systems.[5]

[1] U. Zhao and D. G. Truhlar, *J. Chem. Phys.*, 2006, **125**, 1–17.

[2] Y. Zhao and D. G. Truhlar, *Theor. Chem. Acc.*, 2008, **120**, 215–241.

[3] Y. Zhao and D. G. Truhlar, *Acc. Chem. Res.*, 2008, **41**, 157–167.

[4] M. J. Frisch, G. W. Trucks, H. B. Schlegel, G. E. Scuseria, M. A. Robb, J. R. Cheeseman, G. Scalmani, V. Barone, B. Mennucci, G. A. Petersson, H. Nakatsuji, M. Caricato, X. Li, H. P. Hratchian, A. F. Izmaylov, J. Bloino, G. Zheng, J. L. Sonnenberg, M. Hada, M. Ehara, K. Toyota, R. Fukuda, J. Hasegawa, M. Ishida, T. Nakajima, Y. Honda, O. Kitao, H. Nakai, T. Vreven, J. A. Montgomery, Jr, J. E. Peralta, F. Ogliaro, M. Bearpark, J. J. Heyd, E. Brothers, K. N. Kudin, V. N. Staroverov, R. Kobayashi, J. Normand, K. R aghavachari, A. Rendell, J. C. Burant, S. S. Iyengar, J. Tomasi, M. Cossi, N. Rega, J. M. Millam, M. Klene, J. E. Knox, J. B. Cross, V. Bakken, C. Adamo, J. Jaramillo, R. Gomperts, R. E. Stratmann, O. Yazyev, A. J. Austin, R. Cammi, C. Pomelli, J. W. Ochterski, R. L. Martin, K. Morokuma, V. G. Zakrzewski, G. A. Voth, P. Salvador, J. J. Dannenberg, S. Dapprich, A. D. Daniels, Ö. Farkas, J. B. Foresman, J. V. Ortiz, J. Cioslowski and D. J. Fox, *Gaussian 09*, revision D.01; Gaussian, Inc.: Wallingford, CT, 2009.

[5] W. J. Hehre, R. Ditchfield and J. A. Pople, *J. Chem. Phys.*, 1972, **56**, 2257–2261.